VOLATILE COMPOUNDS IN SHERGOTTITE AND NAKHLITE METEORITES.

James L. Gooding[1], Kwesi E. Aggrey[2,3], and David W. Muenow[2]
[1] SN21/Planetary Science Branch, NASA/Johnson Space Center, Houston, TX 77058. [2] Department of Chemistry and Hawaii Institute of Geophysics, University of Hawaii, Honolulu, HI 96822. [3] School of Theoretical and Applied Science, Ramapo College of New Jersey, Mahwah, NJ 07430.

INTRODUCTION. Since discovery of apparent carbonate carbon in Nakhla [1], significant evidence has accumulated for occurrence of volatile compounds in shergottites and nakhlites. Gooding and Muenow [2] showed that at least one shergottite (EETA79001) contains substantial sulfur in a highly oxidized form and that the oxidation must have occured on the shergottite parent planet. Burgess et al. [3] also found oxidized sulfur in ALHA77005, Shergotty, Nakhla, and Chassigny. Kerridge [4] reported carbon and deuterium of apparent pre-terrestrial origin in Shergotty and Lafayette (a nakhlite). In addition, discrete grains of salt minerals have been documented in EETA79001 and Nakhla [5-7]. Here we present final results from our study of volatile compounds [8] in three shergottites, one nakhlite, and three eucrite control samples.

SAMPLES AND METHODS. Antarctic meteorites included Allan Hills specimens ALHA77005 (shergottite) and ALHA81001 (eucrite), as well as Elephant Moraine specimens EETA79001 (shergottite; lithologies A, B, and C), and EETA79004 (eucrite). A Pasamonte eucrite specimen (USNM-897) was obtained from the U. S. National Museum and a Nakhla specimen (BMNH-1911,369) from the British Museum (Natural History). A Shergotty specimen (GSI-179) was sub-divided from material allocated by the Geological Survey of India to Duke [9]. Samples from the exterior (0-0.5-cm depth, including fusion crust) and interior (> 1-cm depth) of each meteorite were individually analyzed so that terrestrial weathering and contamination could be recognized and not misinterpreted as parent-body effects. Each sample (20-80 mg) was pyrolyzed by continuous heating to 1500 K at 5-6 K/min under 10^{-7} torr vacuum in a Knudsen cell fitted with a high-purity aluminum oxide liner. Evolved gases were analyzed by a quadrupole mass spectrometer that was continuously scanned over m/e = 2-100 to simultaneously measure abundances of H_2O, CO_2, CO, SO_2, S_2, H_2S, HCl, Cl, and hydrocarbons.

RESULTS. *WATER.* For interior samples of shergottites, H_2O-release profiles and total water concentrations (< 0.1%), are not obviously correlated with similar data for other volatile species. A typical H_2O-release profile consists of a single broad peak at 350-700 K that suggests desorption of loosely bound water. Although Nakhla was previously suspected to contain hydrous phases [7,10,11], its measured water content was less than anticipated and its H_2O-release profile was similar to those of shergottites. As discussed below for chlorine, however, it is possible that much of Nakhla's indigenous water reacted to form HCl during pyrolysis. Therefore, the actual water content of Nakhla may be significantly higher than the 0.007% measured as evolved H_2O. Kerridge [4] reported a total of 13.3 ppm H in Shergotty and 58.3 ppm H in the nakhlite, Lafayette, but discarded as terrestrial contamination all gases extracted at < 723 K. Judging from our results for Nakhla, however, HCl evolution (and, by inference, water loss) begins at < 700 K in nakhlites. Therefore, it is possible that Kerridge underestimated the nakhlite water content. *CARBON.* Carbon-containing species included CO_2, CO, and both saturated and unsaturated hydrocarbons (C_1-C_4 compounds). The contrast between exterior and interior samples is not always obvious although there are differences between shergottites/Nakhla, as a group, and eucrites. In addition, comparatively low hydrocarbon contents of Antarctic interior specimens distinguish them from non-Antarctic museum specimens. Evolution of CO_2 from shergottite and Nakhla samples occurs as peaks centered near 750 K or 900 K, the same temperature range over which $CaCO_3$ decrepitates under vacuum [12]. Because $CaCO_3$ has been independently identified as discrete mineral grains in both EETA79001 [5] and Nakhla [7], the evolved CO_2 is attributable to $CaCO_3$. Shergotty shows a surprising abundance of CO_2 but, unlike other shergottite specimens, the CO_2 evolution is closely correlated with the release of hydrocarbons. Therefore, it is likely that some or all of the "apparent carbonate" in Shergotty is associated with terrestrial organic contamination. Two different CO_2 peaks in the Nakhla profile suggest two different CO_2 carriers. Both of the Nakhla carriers must be inorganic, however, because the Nakhla sample in question is virtually free of hydrocarbons. For interior samples of shergottites and Nakhla, there exists an inverse correlation between CO_2 and oxidized sulfur (correlation coefficient, r = -0.71 for 11 samples). Kerridge [4] reported a total of 69.3 ppm C in Shergotty and 112.0 ppm C in Lafayette. His procedure discarded as contamination all gases extracted at < 723 K and interpreted as pre-terrestrial the gases extracted above 1023 K (Lafayette) or 1073 K (Shergotty). Judging from our results for Shergotty and Nakhla, however, Kerridge's procedure might not have excluded some of the hydrocarbon contamination in Shergotty and might have sacrificed some of the carbonate in Nakhla. Our results indicate an intrinsic 210 ppm C in Nakhla.

SULFUR. Most sulfur from interior samples of eucrites, and mildly weathered exterior samples of eucrites, evolves as S_2 with minor H_2S, consistent with a chemically reduced carrier such as pyrrhotite or troilite (FeS). In contrast, large fractions of the sulfur in shergottites and Nakhla evolves as SO_2. The fraction of sulfate in interior samples of eucrites is nearly zero and exhibits a maximum value of about 21% in a moderately weathered interior sample of EETA79004; the fraction of sulfate in shergottite and Nakhla interior samples is 17-100% (Fig. 1). The least oxidized shergottite material is bulk Lith-A from EETA79001 whereas the most oxidized material is Lith-C from the same meteorite; other shergottite and Nakhla samples fall between those limits. Evolution of SO_2 from interior samples of shergottites and Nakhla, which show little evidence of terrestrial weathering, is attributable to decrepitation of indigenous sulfates. Calcium sulfate of apparent pre-terrestrial origin has been independently documented for EETA79001 [5] and both Ca- and Mg-sulfate have been found in Nakhla [6,7]. Evolution of SO_2 from EETA79001/Lith-C is attributable partly to sulfates and partly to a more refractory component that probably occurs as sulfate ions dissolved in glass [2]. In some samples, such as Nakhla, SO_2 evolution at 800-1000 K is correlated with CO_2 evolution. In terms of total abundances, however, CO_2 and SO_2 are inversely correlated, as discussed for carbon results. *CHLORINE.* Most of the chlorine evolved from interior shergottite samples consists of nearly equal concentrations of Cl and HCl although a few samples favor the latter. Exterior samples of terrestrially weathered eucrites, which also contain hydrous weathering products, show HCl as the dominant chlorine species. Therefore, it is likely that HCl evolution from all samples is fostered by pyrolysis reactions involving hydrated phases. Nakhla represents a special case in which HCl and Cl profiles are staggered in temperature, possibly indicating two different chlorine carriers. In addition, evolution of Cl at 800-1150 K is strongly correlated with evolution of monatomic Na (and K). The correlated Cl/Na evolution is attributable to decrepitation of sodium chloride that has been previously identified in Nakhla [6]. Production of HCl can be tentatively attributed to decrepitation of hydrous "rust" that contains trace Cl [7]. For interior samples of shergottites and Nakhla, total chlorine (Cl + HCl) varies inversely with total sulfur but varies directly with the abundance of oxidized sulfur (Fig. 2). No such correlations exist for interior samples of eucrites.

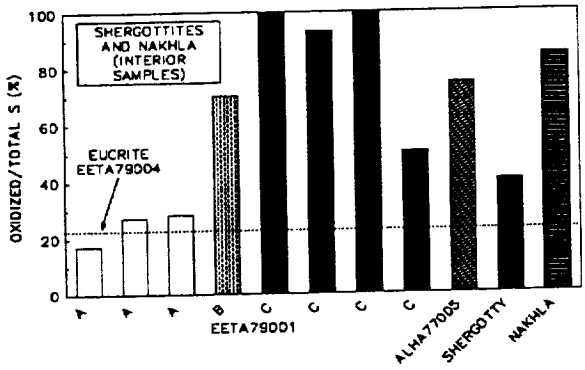

Figure 1. Relative abundances of sulfate in interior samples.

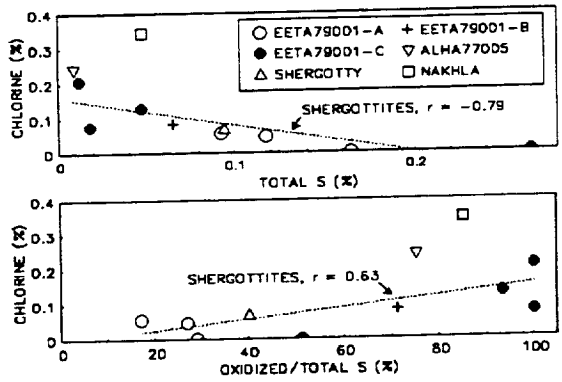

Figure 2. Chlorine-sulfur correlations in interior samples.

CONCLUSIONS. Shergottites ALHA77005, EETA79001, and Shergotty, and the nakhlite Nakhla, all contain oxidized sulfur (sulfate) of pre-terrestrial origin; sulfur oxidation is most complete in EETA79001/Lith-C. Significant bulk carbonate was confirmed in Nakhla and trace carbonate was substantiated for EETA79001, all of which appears to be pre-terrestrial in origin. Chlorine covaries with oxidized sulfur, whereas carbonate and sulfate are inversely related. These volatile compounds were probably formed in a highly oxidizing, aqueous environment sometime in the late-stage histories of the rocks that are now represented as meteorites. They are consistent with the hypothesis that shergottite and nakhlite meteorites originated on Mars and that Mars has supported aqueous geochemistry during its history.

References. [1] Carr R. H. et al. (1985) Nature, 314, p. 248-250. [2] Gooding J. L. and Muenow D. W. (1986) Geochim. Cosmochim. Acta, 50, p. 1049-1059. [3] Burgess R. et al. (1989) Earth Planet. Sci. Lett., 93, p. 314-320. [4] Kerridge J. F.(1988) Lunar Planet Sci. XIX, LPI, Houston, p. 599-600. [5] Gooding J. L. et al. (1988) Geochim. Cosmochim. Acta, 52, p. 909-915. [6] Wentworth S. J. and Gooding J. L. (1988) Lunar Planet. Sci. XIX, LPI, Houston, p. 1261-1262. [7] Wentworth S. J. and Gooding J. L. (1989) Lunar Planet. Sci. XX, LPI, p. 1193-1194. [8] Gooding J. L., Aggrey K. and Muenow D. W. (1987) Meteoritics, 22, p. 191. [9] Duke M. B. (1968) In B. M. French and N. M. Short (Eds.), Shock Metamorphism of Natural Materials, Mono, Baltimore, p. 613-621. [10] Ashworth J. R. and Hutchison R. (1975) Nature, 256, p. 714-715. [11] Bunch T. E. and Reid A. M. (1975) Meteoritics, 10, p. 303-315. [12] Kotra R. K. et al. (1982) Icarus, 51, p. 593-605.

VALLEY DEVELOPMENT ON MARS: A GLOBAL PERSPECTIVE; V.C. Gulick and V.R. Baker, Departments of Geosciences and Planetary Sciences, University of Arizona, Tucson, Arizona 85721.

Several periods of fluvial valley activity have so far been documented on Mars. These periods span Mars' geologic history with widespread episodes occurring during the Noachian, and localized episodes continuing into the Hesperian and Amazonian (Figure 1). Each fluvial event produced valleys which are distinct in overall morphology and network pattern, therefore providing information about the environment in which they formed. The formational environments required are consistent with those in the global model presented by Baker *et al.* [1].

By far the most widespread fluvial valley development is located in the heavily cratered uplands. These valleys form laterally extensive networks which are highly degraded. Headwater regions frequently cannot be traced with the quality of the existing images [2]. However, in areas where they can be traced, tributaries often originate on crater slopes. Lower reaches appear buried and later reactivated by the formation of less extensive pristine valleys in the intercrater plains. The resulting degraded and pristine compound valley morphology has important implications for the environment in which they formed. Because the degraded networks are more laterally extensive and have relatively higher drainage densities than the pristine networks [2], more water was probably available at the surface during the period when the degraded networks formed. In contrast, the pristine valleys which formed in the intercrater plains units appear to be structurally controlled. These networks seem to follow either pre-existing valleys (*e.g.* Margaritifer Sinus Region) or underlying fracture patterns (*e.g.* Nirgal Vallis, Nanedi Vallis) suggesting a subsurface water source was more important in the formation of these valleys.

Fluvial valleys are also present on Ceraunius Tholus and Hecates Tholus [3,4], two Noachian age volcanoes located in the northern plains region [5]. These valleys have drainage densities that are one to two orders of magnitude higher than those in the southern highlands and are equivalent to drainage densities of terrestrial runoff valleys [3,4]. Valleys on Ceraunius and Hecates exhibit a similar compound network morphology as the Noachian valleys in the southern highlands. However, the pristine valley segments on Ceraunius and Hecates are not structurally controlled, in that they do not follow pre-existing fractures. Instead they have exploited and subsequently enlarged or reactivated pre-existing fluvial valleys.

The overall morphology of valleys formed on Noachian age surfaces seems to suggest that surface runoff was at least initially important in the formation of the degraded valleys. However, these valleys probably never developed into highly integrated valley systems, because of the relatively high permeablity of the Martian surface. With the emplacement of the intercrater plains, the style of valley formation changed to a more sapping dominated system where pre-existing valleys or fracture systems provided the locus for subsequent valley formation. Carr [6] noted that the rates of early valley development correlate with cratering rates. We add that the style of valley formation is also consistent with declining impact rates. Cratering rates were still fairly high when the degraded valleys were forming, releasing much of the trapped subsurface water into the surface environment and producing runoff in regions where surface permeabilities were low enough. At any given crater, surface water was probably initially fairly plentiful as a result of vigorous impact-induced hydrothermal circulation [7,8]. With time, hydrothermal circulation became increasingly restricted to the subsurface environment and valley development continued largely as a result of subsurface sapping processes. If the emplacement of the intercrater plains was at least partly volcanic in nature (the result of subsurface magmatic activity *e.g.*, sill intrusions) as suggested by Wilhelms and Baldwin [9], then even longer ($\geq 10^6$ years) hydrothermal circulation would be produced [8]. Near surface aquifers would be recharged with warm, upwardly migrating mineral-rich water and sapping processes would proliferate, reactivating existing valleys or forming new ones where underlying fractures and ground- water flow intersected with the surface environment. Some of this water would be lost to the atmosphere but much of it would infiltrate back into the permeable subsurface in local ice-free regions.

While widespread valley development on Mars ceased soon after the end of heavy bombardment, local areas of fluvial valley activity continued into the Hesperian in the Tempe, Electris and Casius regions [10] and probably also in the Mangala Vallis region [11]. Valley development in these regions appears to be controlled

largely by fractures. Valleys are enlarged, flat-floored and have extremely low drainage densities [10] which is consistent with a sapping origin. These networks probably formed initially as a result of locally intense volcanic activity [10]. Since these valleys are all located near the shore of the putative ocean, subsequent aquifer recharge could have been provided by earlier episodes of outflow channel discharges. The period of ancient glaciation [12] in the southern hemisphere appears to have occurred during this time.

The latest period of fluvial valley development documented so far occurred on the northern flank of Alba Patera. These valleys are Amazonian in age and are morphologically similar to those formed by rainfall-runoff processes on the Hawaiian volcanoes [3,4]. According to the model presented in Baker *et al.* [1], the last major episode of ancient ocean formation resulting from outflow channel discharges was relatively short-lived ($\leq 10^4$ years) and is concurrent with the formation of the Alba valleys [3,4]. Thus the brevity of this episode and the generally high Martian surface permeabilites precluded the formation of fluvial runoff valleys by atmospheric precipitation in all regions except in the lowest permeability, easily eroded zones on Alba Patera [3,4].

REFERENCES [1] Baker, V.R. *et al.* (1990), *LPSC XXI.*; [2] Baker, V.R. and Partridge, J.B. (1986) *J. Geophys. Res.* **91**, 3561–3572. [3] Gulick, V.C. and Baker, V.R. (1989) *Nature* **341**, 514–516. [4] Gulick, V.C. and Baker, V.R. (in press) *J. Geophys. Res.* [5] Barlow, N.G. (1989) *Icarus* **75**, 285–305. [6] Carr, M.H. (1989) *Icarus* **79**, 311–327. [7] Brakenridge *et al.* (1985) *Geology* **13**, 859–862. [8] Gulick *et al.* (1988) *LPSC XIX*, 441–442. [9] Wilhelms, D.E. and Baldwin, R.J. (1989) *LPSC XIX Proc.*, 355–365. [10] Grant, J.A. and Schultz, P.M. (1989) *NASA Tech. Memo.* **4130**, 382–383. [11] Chapman, M.G. *et al.* (1989) *USGS Map I-1962.* [12] Kargel, J. and Strom R. (1990), *LPSC XXI.*

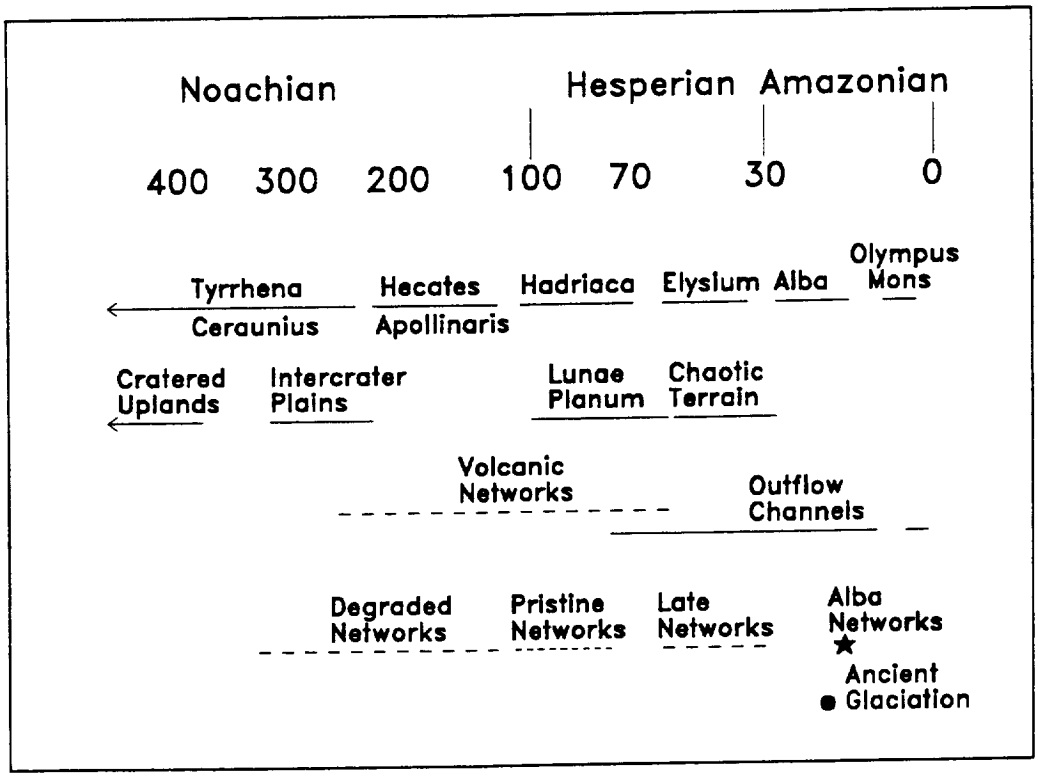

Figure 1. Relative ages of volcano, valley, and channel formation in Mars' history. Numbers represent crater densities, where crater density is defined as the number of craters $\geq$ 8 km diameter/10^6 km^2. Relative age data (crater densities) of volcanoes and terrain units taken from Barlow [5]. Relative age of ancient glaciation taken from Kargel and Strom [12]. Figure modified from Gulick and Baker [4].

MORPHOMETRY OF FRESH IMPACT CRATERS IN HESPERIA PLANUM, MARS: Joan Hayashi-Smith and Peter J. Mouginis-Mark, Planetary Geosciences Division, SOEST, University of Hawaii, Honolulu, HI 96822.

INTRODUCTION: We explore a concept originally proposed by Cintala and Mouginis-Mark (1) that martian impact craters display a gradual transition with increasing crater size from larger depth/diameter ratios at small diameters to lower values for larger craters. This correlation was interpreted to be the consequence of a pronounced stratification of volatiles within the target. Recent developments in the ability to use PICS software to make quantitative measurements of crater geometry have enabled us to test the hypothesis using craters located in a single region of Mars on the ridged plains materials of Hesperia Planum (~21 - 34°S, 233 - 248°W).

The origin of the ridged plains materials and their thickness within Hesperia Planum are currently unknown. Because of their similarity to the lunar maria, it is likely, however, that these materials comprise a series of flood lavas that partially infilled topographic depressions within the martian highlands. Measurements of crater diameter and the preserved heights of partially buried crater rims, provide estimates that these lava flows within Hesperia Plánum are between 200 - 400 meters thick (2). What is not clear is the spatial distribution of flow thickness or the physical characteristics of the buried terrain.

SHADOW MEASUREMENTS: Our sample contains 61 craters in the diameter range 2.00 - 48.72 km. Of these craters, 26 are morphologically very fresh, possessing complete rims, well preserved ejecta blankets with radial striations or sharp distal ramparts, and have no superposed impact craters. These freshest craters are 2.44 - 14.28 km in diameter, and are used here to investigate the possible role of volatiles in influencing impact crater geometry. Crater depth/diameter measurements were made using digital versions of the Viking Orbiter images and the PICS image processing software (Fig. 1). The resolution of each frame (~95 m/pixel) and the lighting geometry (incidence angle = 64 - 72°) of the crater center were used to convert measurements, in the number of pixels, into distances and shadow lengths and, hence, rim heights. Visual analysis of these images identified that some of the SEDR solar azimuth angle files are incorrect, so that we estimated the solar azimuth (i.e., the perpendicular to rim shadows for near-circular impact craters) for each frame. The average of three crater diameters was used for each crater, one diameter being measured in the same direction as the sun angle and two at about ± 45° to the solar azimuth. In all cases, the rim crest of the crater was taken to be the point where there was a rapid variation in the data number (DN) values (in PICS this typically corresponded to a change of 3 - 5 times the variation observed for illuminated terrains). The rapid increase in DN values was also used to determine the edge of the shadow and, from simple trigonometry, the height of the crater rim. For a few of the craters larger than ~4 km diameter, it was also possible to obtain measurements of the height of the far rim above the surrounding terrain (Fig. 2).

DISCUSSION: The original premise (1) was that sub-surface volatiles had a variable distribution with depth beneath the surface, but that either water or ice was distributed in fixed proportions over the age of the exposed surface. Clearly, as it is likely that volatiles were driven towards the poles over martian history (3), this concept of a constant volatile concentration with depth is unlikely to be valid. Our preliminary analysis of the Hesperia Planum craters fails to identify the gradual transition from small craters formed within a shallow (top 100 m?) permafrost layer within the target to larger craters formed with deeper, volatile-poor, strata below the permafrost (perhaps at depths of a few hundred meters). Based on our estimates of depth and rim height, several of the freshest craters would penetrate the entire 400 m thickness of the ridged plains materials (Fig. 3), excavating the crater floor within the basement materials. Although ejecta deposits are likely to originate from within the near-surface layers (based on analogy with the ejecta deposits associated with Ries Crater in West Germany; ref. 4), the slumping of the inner wall of the crater and the degree of floor rebound may be significantly affected by this strong stratification of the target materials. Although we cannot at this time identify the reason for this disparity between our results and earlier ideas (1), we offer two possible explanations:

1) Cintala and Mouginis-Mark (1980) measured craters on a variety of geological units, some of which may have contained fewer volatiles than did other units.

2) Our analysis has concentrated on the youngest, best-preserved craters within Hesperia Planum, specifically to avoid complications in crater geometry that may have been caused by erosion or subsequent infilling. Our criteria for recognizing these craters will thus bias our sample to preferentially include only the most recent craters, which may have formed at a time when the ridged plains materials of Hesperia Planum had become dessicated. By studying craters of different degradation states, it may still be possible to investigate the temporal evolution of the hypothesized volatile layer provided that subaerial modification processes can be accounted for.

REFERENCES: 1) Cintala, M.J. and Mouginis-Mark, P.J. (1980). Geophys. Res. Lttrs. 7, p. 329 - 332. 2) De Hon, R. A. (1985). Rpt. Plan. Geol. Prog., 1984, NASA TM-87563, p. 242 - 244. 3) Fanale, F.P.et al. (1986). Icarus, **67**, p. 1 - 18. 4) Horz, F. et al. (1983). Revs. Geophys. Space Phys., **21**, p. 1667 - 1725.

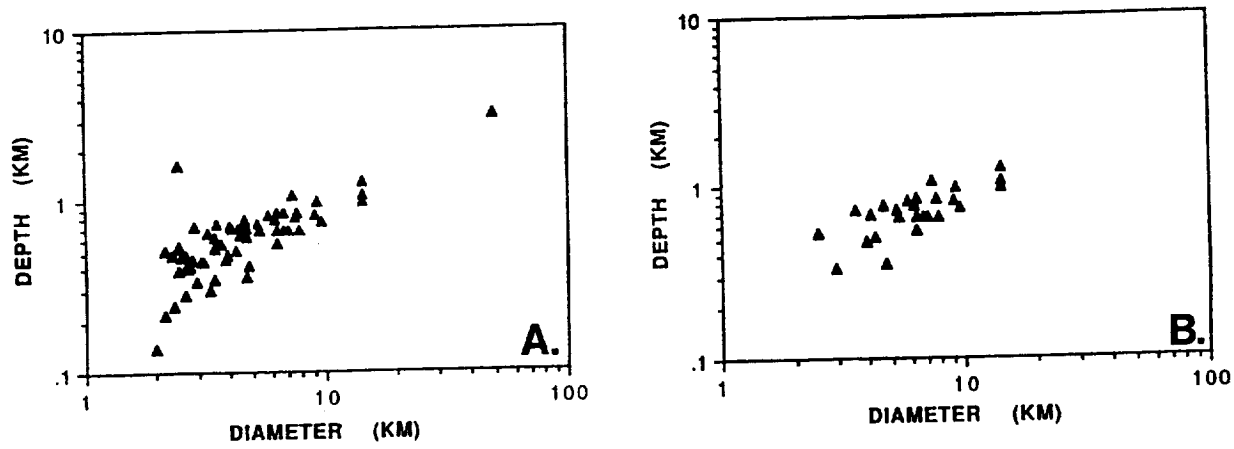

Fig. 1 A) Depth - diameter plot of all craters measured in this analysis. B) Depth - diameter plot of only those craters considered to be "pristine" in this analysis.

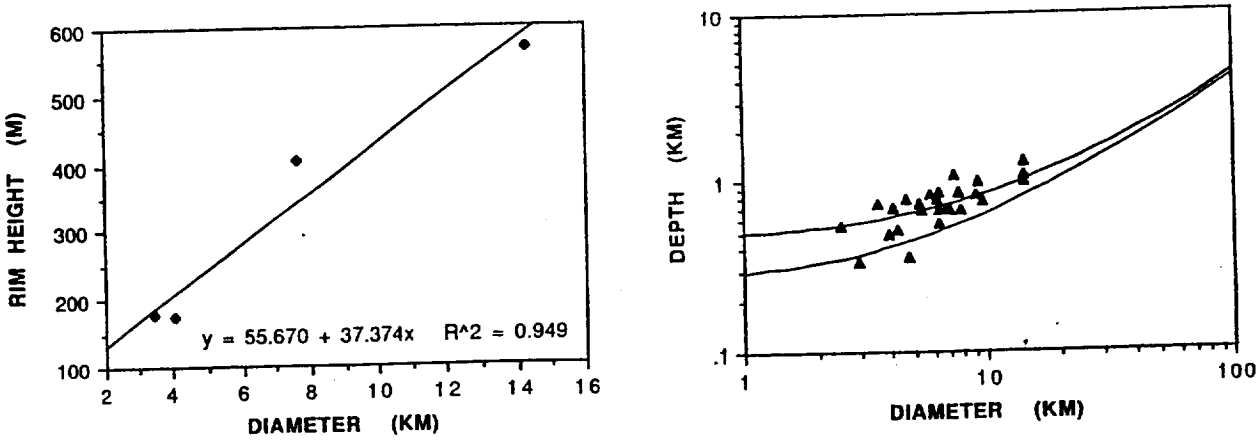

Fig. 2 (Left) Four of the studied craters possess measurable rim heights, permitting a linear least squares fit and, hence, the rim height to crater diameter relationship to be obtained. Fig. 3 (Right) Using the relationships between depth (Fig. 1) and rim height (Fig. 2) to crater diameter, the minimum depth of a crater that is required to penetrate the average thicknesses of the ridged plains materials can be inferred (2). Bottom curve - 200 m; top curve - 400 m plains thickness.